INT. J. RADIAT. BIOL 2002, VOL. 78, NO. 7, 605–609

Taylor&Francis
healthsciences

Alpha-particle lineal energy spectra for the human lung

D. NIKEZIC† and K. N. YU*

(Received 14 September 2001; accepted 6 December 2001)

Abstract.
Purpose: To determine the distribution of lineal energy in the target cells and the parameters of distribution for various combinations of sources, targets and energies in the human tracheobronchial tree. Frequency average and average of the square of the lineal energy were also calculated from the lineal energy distribution.
Method: A model was created to simulate the geometric distribution of cell nuclei in the airway of the tracheobronchial tree. Propagation of alpha particles in such a model was simulated by the Monte Carlo method. Microdosimetric distributions of lineal energy were calculated.
Results: Distributions of lineal energy were substantially different for basal and secretory cells. The frequency average of specific energy was found to be between 0.3 Gy and 0.4 Gy.
Conclusions: Interactions of alpha particles with basal and secretory cells show significant differences: events with small energy transfer are dominant for basal cells, while those with large transfer are dominant for secretory cells. This finding can influence dose weightings and yield lower values of the dose-to-exposure coefficient.

1. Introduction

Alpha particles emitted by radon progeny deposited on inner surfaces of airway tubes in the human lung damage the radiosensitive target cells and give rise to pathological changes. Calculation of the dose absorbed in sensitive cells has been a subject of many studies (Harley 1984, James 1984, NRC 1991, Birchall and James 1994, ICRP 1994, Porstendörfer and Reineking 1999, Marsh and Birchall 2000). Both secretory and basal cells are considered sensitive to alpha radiation. Radiation doses are usually calculated separately for these cells, which are then averaged and weighted throughout the tracheobronchial (T-B) tree.

The most recent dosimetric lung model is that published by the International Commission on Radiological Protection in their ICRP66 report (ICRP 1994). In their approach, dose is calculated in layers containing the sensitive cells by assuming that the dose values in the sensitive cells are the same as those in the layers. Another possible approach is the microdosimetric method, which calculates distributions of microdosimetric quantities in the human lung (Hui *et al.* 1990, Caswell *et al.* 1994, Hofmann *et al.* 1994, Sedlak 1996, Zaider and Varma 1996, Hofmann *et al.* 2000). The most important microdosimetry quantities are the specific energy z and lineal energy y. The specific energy is defined as the ratio of energy ε imparted by radiation to the mass m of the absorber (Kellerer 1985, Rossi and Zaider 1996). The unit of specific energy is J/kg or Gy. The lineal energy is defined as the ratio of energy ε imparted to the average chord length. Both quantities are stochastic and highly variable.

The present work considers the irradiation of basal and secretory cell nuclei in the wall of an airway tube in the T-B tree by alpha particles emitted from short-lived radon progeny and calculates the lineal energy distributions. All calculations were performed using the morphometric model of the human lung and airway wall proposed by ICRP (1994) and NRC (1991).

2. Methods

Monte Carlo simulations of the propagation of alpha particles were performed to calculate lineal energy distributions. Only the most important features of the computer program will be described here. The model consists of two parts, namely the geometrical and the physical sub-models. The physical sub-model is related to the stopping power of alpha particles in striated tissue and air, which are based on the data given in the ICRU49 (ICRU 1993); the dependence of stopping power on the energy of alpha particles is given in ICRU49. These data were fitted and converted into tables where the energy E and the stopping power S are given as functions of the distance d traveled by the alpha particles. The functions $S(d)$ and $E(d)$ are given in the tables in steps of distance; the S and E between two discrete values of d were found by linear interpolation. Calculations of E and S have been performed with the continuous slowing down approximation (or CSDA).

Monte Carlo simulation requires a well-defined

*Author for correspondence; e-mail: peter.yu@cityu.edu.hk
Department of Physics and Materials Science, City University of Hong Kong, Tat Chee Avenue, Kowloon Tong, Kowloon, Hong Kong.
†On leave from University of Kragujevac, Faculty of Science, 34000 Kragujevac, Yugoslavia.

International Journal of Radiation Biology ISSN 0955-3002 print/ISSN 1362-3095 online © 2002 Taylor & Francis Ltd
http://www.tandf.co.uk/journals
DOI: 10.1080/09553000210123694

geometrical model in which the transport of particles is considered. A model of airway tubes and walls described by ICRP66 (ICRP 1994) and NRC (1991) was adopted. Starting points of alpha particles were sampled in the mucus layer in which alpha emitters are distributed. The thickness of the mucus layers are 5 μm in the fast and 6 μm in the slow clearance phase in the bronchial region (BB), and 2 μm in the fast and 4 μm in the slow clearance phase in the bronchiolar region (bb). In the ICRP66 approach, the dose is calculated for the layer containing sensitive cells, thus neglecting their distribution and abundance. Information on distribution and relative volume abundance of sensitive cells was given by Mercer *et al.* (1991). In the present work, the authors have applied the ICRP66 geometrical model but adopted the volume abundance of sensitive-cell nuclei given by Mercer *et al.* (1991). The radius of a cell nucleus is 4.5 μm in the BB region of the T-B tree and 4 μm in the bb region. The cell nuclei are taken to be uniformly and randomly distributed in the sensitive-cell layer as proposed by ICRP66.

The first step in the program is the *construction* of cell nuclei in a given layer according to their volume abundance as given by Mercer *et al.* (1991). The number of nuclei is computed through division of the volume of the layer by the volume abundance. These nuclei are programmed to randomly distribute within the layer and their positions are stored in the computer memory.

The second step is the *creation* of alpha-particle histories and examination of possible hits of cell nuclei. In case of a hit, the energy ε imparted to a nucleus is calculated based on the incident energy and other relevant geometrical parameters. The distance from the emission point to the nucleus (in tissue equivalent form) and the chord length through the nucleus must be known in order to calculate ε. The lineal energy is calculated as the ratio of ε/l_{av}. The procedure was repeated until 10^4 successful histories were achieved. The frequency averages of the specific and lineal energy, and lineal energy distributions could then be obtained.

The model with a random distribution of cell nuclei used for the calculations is shown in figure 1. Panel (a) shows the cross-section of the airway wall, with cell nuclei represented by solid circles and randomly distributed in the layer containing basal or secretory cells. A number of alpha-particle tracks are schematically illustrated by arrows. Particle 3 has a glancing hit on a cell nucleus with a small energy imparted to the nucleus, while particle 4 has a head-on hit with a larger energy imparted to the nucleus. Panel (b) shows a three-dimensional sketch of the model.

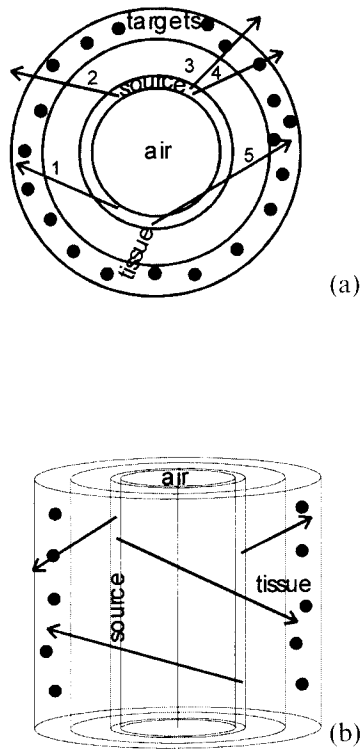

Figure 1. Geometrical model of airway tube and schematic representation of alpha-particle tracks; sensitive cells are randomly distributed. (a) Cross-section of the tube; (b) three-dimensional representation.

3. Results and conclusions

Calculations have been performed for the various source–target combinations listed below. The sources include fast and slow mucus in BB and bb. The targets are nuclei of basal and secretory cells in BB, and of secretory cells in bb. The y-spectra are the plots of $yf(y)$ (as the y-axis; dimensionless) against the lineal energy y (as the x-axis with a logarithmic scale; in keV/μm). The y-spectra have been obtained for each combination of sources and targets for the two alpha-emitting nuclides in the radon chain, i.e. ^{218}Po and ^{214}Po. Results of these calculations are given in figures 2, 3 and 4.

Figure 2 gives results for secretory-cell nuclei in BB. Strongly expressed maxima appeared between 150 and 250 keV/μm. It is interesting to note that the trends appear as doublets: the trend for alpha particles emitted with an initial energy of 7.69 MeV in fast mucus is close to that for 6 MeV and slow mucus; and those for 7.69 MeV and slow mucus is close to that for 6 MeV and fast mucus.

Figure 3 shows the results for basal-cell nuclei in BB. Peaks are completely missing above 100 keV/μm for alpha particles of 6 MeV, and weakly expressed for alpha particles of 7.69 MeV. Comparison between

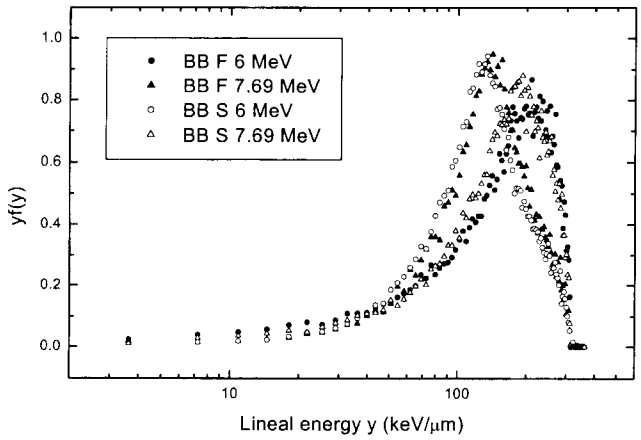

Figure 2. Lineal energy (y) spectra for secretory-cell nuclei in the bronchial region.

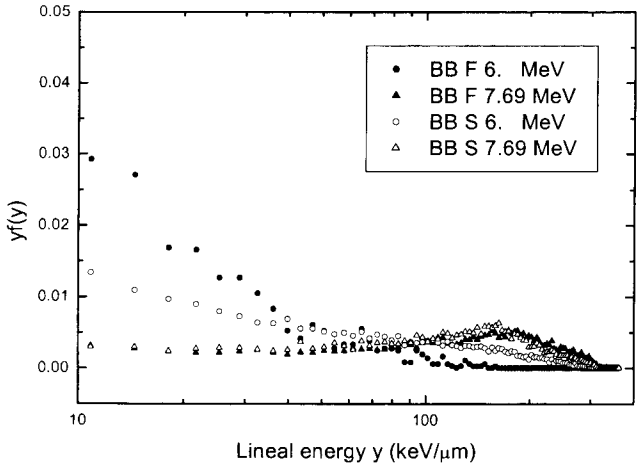

Figure 3. Lineal energy (y) spectra for basal-cell nuclei in the bronchial region.

figures 2 and 3 reveals remarkably different interactions of alpha particles with basal-cell and secretory-cell nuclei in BB. The conclusion is that small energy transfer events dominate the interactions with basal-cell nuclei, while large energy transfer events dominate those with secretory-cell nuclei.

Figure 4 shows results for secretory-cell nuclei in bb. The trends appear in doublets again, but this time the trends for the same alpha energy pair up. The peaks at about 110 and 150 keV/μm for 7.69 MeV and 6 MeV, respectively, are very strongly expressed. When compared with figure 2, it can be seen that the peaks are shifted towards smaller values of y. This is explained by the smaller distance between the alpha-particle sources and the targets, and thus larger average entry alpha energy in the cell nuclei (which implies smaller stopping power) in bb.

Parameters of the distributions shown in figures 2, 3 and 4 are summarized in table 1. The first three

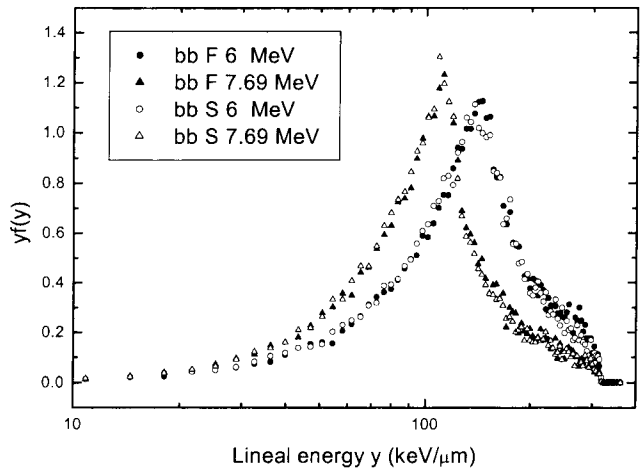

Figure 4. Lineal energy (y) spectra for secretory-cell nuclei in the bronchiolar region.

columns give the source, target and energy of alpha particles. The fourth and fifth columns give the frequency average of the lineal energy $\bar{y}_F$ and its squared value $\bar{y}_F^2$, respectively. The sixth column gives the frequency average of the specific energy $\bar{z}_F$ calculated from

$$\bar{z}_F = \frac{\bar{y}_F}{\pi \rho r^2}$$

where $\rho = 1.045\,\mathrm{g/cm^3}$ is the density of the tissue and r is the radius of a cell nucleus. One line of data (BB fast 6 MeV $\rightarrow$ basal) is very different from the others. This difference occurs because basal cells are close to the end of range of alpha particles emitted with 6 MeV energy (by ^{218}Po) in fast mucus.

Determination of the absorbed dose D in the sensitive targets requires a knowledge of the fraction F of nuclei hit by alpha particles for a given exposure condition. The absorbed dose is given by $D = F \times \bar{z}_F$. A dosimetric lung model as well as defined exposure conditions are needed to determine F, which is beyond the scope of this paper. The specific energy for basal cells for alpha energies of 6 MeV is significantly smaller. In all other cases the average specific energies are between 0.3 Gy and 0.4 Gy.

Distributions of lineal energy in the T-B tree were previously determined by Caswell *et al.* (1994) for both ^{218}Po (with alpha energy 6 MeV) and ^{214}Po (with alpha energy 6 MeV). In that work, the Yeh and Schum (1980) morphometry model was used, while in the present work models of airway walls and the morphometry model according to ICRP66 (ICRP 1994) were adopted, and more realistic distributions of target-cell nuclei were employed. Caswell *et al.* (1994) calculated the distributions of lineal energy for cell depths from 10 μm to 70 μm and for airway

Table 1. Parameters of microdosimetric distributions.

Source	Target cell	Energy (MeV)	$\bar{y}_F$ (keV/μm)	$\bar{y}_F^2$ (keV/μm)^2	$\bar{z}_F$ (Gy)
BB fast	Secretory	6	143.3	191.9	0.345
BB fast	Secretory	7.69	130.0	162.8	0.313
BB slow	Secretory	6	145.9	156.9	0.351
BB slow	Secretory	7.69	124.3	186.3	0.299
BB fast	Basal	6	27.8	55.8	0.067
BB fast	Basal	7.69	149.7	191.3	0.361
BB slow	Basal	6	83.72	143.4	0.201
BB slow	Basal	7.69	136.9	174.7	0.330
bb fast	Secretory	6	128.0	157.9	0.390
bb fast	Secretory	7.69	103.0	129.8	0.314
bb slow	Secretory	6	124.8	154.1	0.387
bb slow	Secretory	7.69	101.3	127.2	0.308

diameters 1.130, 0.651, 0.435, and 0.198 cm (generations 2, 4, 6 and 10 of the Yeh and Schum morphometry). In the present work, the authors calculated distributions for different regions of the T-B tree (namely the fast and slow mucus layers in the bronchial region (BB) and the bronchiolar region (bb)), and for cells distributed randomly in the wall of the airway.

Despite the many different considerations between the present investigation and that of Caswell *et al.* (1994), they gave results that generally compare well with those of the present authors. These include the lineal energy spectra for ^{218}Po and ^{214}Po at various depths for generation 2 of the Yeh Schum morphometry (see their figures 4 and 5) and the lineal energy spectra for ^{214}Po for various airway generations for a cell depth of 30 μm. The first observation is that the shapes of the lineal energy spectra are in general similar to the present authors' results, in particular for those of secretory cells. Caswell *et al.* (1994) demonstrated that the lineal energy distributions were extended up to around 360 keV/μm and possessed maxima between 100 and 200 keV/μm, which are also consistent with the present findings.

According to ICRP66 (ICRP 1994), doses are separately calculated in basal cells (D_{bas}) and secretory cells (D_{sec}). Subsequently, the dose in the bronchial region (D_{BB}) is calculated as $D_{BB} = 0.5D_{bas} + 0.5D_{sec}$. In other words, doses are weighted with an equal weighting factor of 0.5. Such an approach assumes equal sensitivity of basal and secretory cells to alpha radiation (see also NRC 1999). This assumption was required mainly because there was not enough information regarding the relative sensitivity of basal and secretory cells. However, as shown in the present work, interactions between alpha particles with basal and secretory cells are different, so these weighting factors should also be different. In the opinion of the authors, the weighting factor for basal cells should be larger than that for secretory cells because basal cells are subjected to more hits with small energy transfer, which can be more efficient in cancer initiation. In contrast, secretory cells suffer from more hits with large energy transfer, which might be lethal and less efficient in cancer production. Since the dose in basal cells is much smaller than that in secretory cells, a heavier weighting for basal cells will bring down the calculated dose in the respiratory tract. Having presented the above reasoning, it should also be remarked here that they are all referring to direct irradiation of cells or cell nuclei. Over the past ten years there have been reports of the bystander effect, in which unirradiated cells can also suffer biological consequences when they are in the presence of irradiated cells (Nagasawa and Little 1992, Deshpande *et al.* 1996, Sigg *et al.* 1997, Azzma *et al.* 1998, Mothersill and Seymour 1998, Bishayee *et al.* 1999). The dependence of the bystander effect to the amount of energy transfer per alpha hit, and thus its influence on the weighting factor for secretory and basal cells, is the subject of future investigations.

Acknowledgement

The present research was supported by the CERG grant CityU1004/99P from the Research Grant Council of Hong Kong.

References

Azzma, E. I., de Toledo, S. M., Gooding, T. and Little, J. B., 1998, Intercellular communication is involved in the bystander regulation of gene expression in human cells exposed to very low fluences of alpha particles. *Radiation Research*, **150,** 497–504.

Birchall, A. and James, A. C., 1994, Uncertainty analysis of the effective dose per unit exposure from radon progeny

and implication for ICRP risk-weighting factors. *Radiation Protection Dosimetry*, **53,** 133–140.

Bishayee, A., Rao, D. V. and Howell, R. W., 1999, Evidence for pronounced bystander effects caused by nonuniform distributions of radioactivity using a novel three-dimensional tissue culture model. *Radiation Research*, **152,** 88–97.

Caswell, R. S., Karam, L. R. and Coyne, J. J., 1994, Systematics of alpha-particle energy spectra and lineal energy (Y) spectra for radon daughters. *Radiation Protection Dosimetry*, **52,** 377–380.

Deshpande, A., Goodwin, E. H., Bailey, S. M., Marrone, B. L. and Lehnert, B. E., 1996, Alpha-particle-induced sister chromatid exchange in normal human lung fibroblast—evidence for an extranuclear target. *Radiation Research*, **145,** 260–267.

Harley, N. H., 1984, Comparing radon daughter dose: underground vs. environment exposure. *Radiation Protection Dosimetry*, **7,** 371–375.

Hofmann, W., Menache, M. G., Crawford-Brown, D. J., Caswell, R. S. and Karam, L. R., 2000, Modeling energy deposition and cellular radiation effects in human bronchial epithelium by radon progeny alpha particles. *Health Physics*, **78,** 377–393.

Hofmann, W., Nosterer, M., Menache, M. G., Crawford-Brown, D. J., Caswell, R. S. and Coyne, J. J., 1994, Microdosimetry and cellular radiation effects of radon progeny in human bronchial airways. *Radiation Protection Dosimetry*, **52,** 381–385.

Hui, T. E., Poston, J. W. and Fisher, D. R., 1990, The microdosimetry of radon decay products in the respiratory tract. *Radiation Protection Dosimetry*, **31,** 405–411.

ICRP (International Commission on Radiological Protection), 1994, Human respiratory tract model for radiological protection. A report of a Task Group of the International Commission on Radiological Protection. ICRP Publication 66 (New York: Pergamon Press).

ICRU (International Commission of Radiation Units and Measurements), 1993, Stopping powers and ranges for protons and alpha particles. ICRU Report 49 (Maryland: International Commission of Radiation Units and Measurements).

James, A. C., 1984, Dosimetric approaches to risk assessment for indoor exposure to radon daughters. *Radiation Protection Dosimetry*, **7,** 353–366.

Kellerer, A. M., 1985, Fundamentals of microdosimetry. In *The Dosimetry of Ionizing Radiation*, Vol. 1, edited by K. R. Kase, B. E. Bjongard and F. H. Attix (Orlando: Academic Press), pp. 78–162.

Marsh, J. W. and Birchall, A., 2000, Sensitivity analysis of the weighted equivalent lung dose per unit exposure from radon progeny. *Radiation Protection Dosimetry*, **87,** 167–178.

Merger, R. R., Russel, M. L. and Crapo, J. D., 1991, Radon dosimetry based on the depth distribution of nuclei in human and rat lungs. *Health Physics*, **61,** 117–130.

Mothersill, C. and Seymour, C. B., 1998, Cell–cell contact during gamma irradiation is not rquired to induce a bystander effect in normal kidney keratinocytes: evidence for release during irradiation of a signal controlling survival into the medium. *Radiation Research*, **149,** 252–262.

Nagasawa, H. and Little, J. B., 1992, Induction of sister chromatid exchanges by extremely low doses of alpha-particles. *Cancer Research*, **52,** 6394–6396.

NRC (National Research Council), 1991, Comparative dosimetry of radon in mines and homes. Panel on dosimetric assumption affecting the application of radon risk estimates (Washington DC: National Academy Press).

NRC (National Research Council), 1999, Health effects of exposure to radon: BEIR VI (Washington DC: National Academy Press).

Porstendörfer, J. and Reineking, A., 1999, Radon: characteristics in air and dose conversion factors. *Health Physics*, **76,** 300–305.

Rossi, H. and Zaider, M., 1996, *Microdosimetry and its Applications* (Berlin: Springer).

Sedlak, A., 1996, Microdosimetric approach to the problem of lung cancer induced by radon progeny. *Health Physics*, **70,** 680–688.

Sigg, M., Crompton, N. E. A. and Burkhart, W., 1997, Enhanced neoplastic transformation in an inhomogeneous radiation field: an effect of the presence of heavily damaged cells. *Radiation Research*, **148,** 543–547.

Yeh, H. C. and Schum, G. M., 1980, Model of human lung airways and their application to inhaled particle deposition. *Bulletin of Mathematical Biology*, **42,** 461–480.

Zaider, M. and Varma, M., 1996, Carcinogenic risk coefficients at environmental levels of radon exposures: a microdosimetric approach. *Health Physics*, **70,** 837–844.